

1
2

3

4 **Expression of the ACE2 virus entry protein in the nervus terminalis suggests**
5 **an alternative route for brain infection in COVID-19**

6

7 **Katarzyna Bilinska¹, Christopher S. von Bartheld² and Rafal Butowt^{1*}**

8

9

10 ¹ L. Rydygier Collegium Medicum, Nicolaus Copernicus University, Bydgoszcz,
11 Poland

12 ² Department of Physiology and Cell Biology, University of Nevada, Reno School of
13 Medicine, Reno, NV, United States

14

15

16

17

18 **Number of words in text:** 2,995

19 **Number of Figures:** 4

20 **Number of Tables:** 0

21

22 **Key words:** Nervus terminalis, ACE2, SARS-CoV-2, COVID-19, brain infection,
23 olfactory system

24 **Abstract**

25

26 Previous studies suggested that the SARS-CoV-2 virus may gain access to the brain
27 by using a route along the olfactory nerve. However, there is a general consensus that
28 the obligatory virus entry receptor, angiotensin converting enzyme 2 (ACE2), is not
29 expressed in olfactory receptor neurons, and the timing of arrival of the virus in brain
30 targets is inconsistent with a neuronal transfer along olfactory projections. We
31 determined whether nervus terminalis neurons and their peripheral and central
32 projections may provide an alternative route from the nose to the brain. Nervus
33 terminalis neurons were double-labeled with antibodies against ACE2 and nervus
34 terminalis markers in postnatal mice. We show that most nervus terminalis neurons
35 with cell bodies in the region between the olfactory epithelium and the olfactory bulb
36 express ACE2, and therefore may provide a direct route for the virus from the nasal
37 epithelium and Bowman's glands to brain targets, including the telencephalon and
38 diencephalon.

39

40

41

42 **INTRODUCTION**

43 Many previous reports have suggested that the severe acute respiratory syndrome
44 coronavirus 2 (SARS-CoV-2) gains access to the brain by using an olfactory route from
45 the nose to the brain (Bougakov et al., 2020; Briguglio et al., 2020; Butowt and Bilinska,
46 2020; Li et al., 2020; Meinhardt et al., 2020; Natoli et al., 2020; Zubair et al., 2021;
47 Burks et al., 2021), similar to other neuro-invasive viruses that have been shown to
48 infect olfactory receptor neurons and spread from these first-order olfactory neurons to
49 secondary and tertiary targets in the brain (Barnett and Perlman, 1993; van Riel et al.,
50 2015; Dubé et al., 2018). Indeed, it has been shown that SARS-CoV-2 can accumulate
51 in various brain regions, in animal models (reviewed in: Butowt and von Bartheld, 2020;
52 Rathnasinghe et al., 2020) and in a small number of human patients with COVID-19
53 (Ellul et al., 2020; Matschke et al., 2020; Meinhardt et al., 2020; Mukerji and Solomon,
54 2020; Solomon, 2021).

55

56 However, the route along the olfactory nerve from the nose to the brain is controversial
57 for SARS-CoV-2, primarily for two reasons: (1) the olfactory receptor neurons do not
58 express the obligatory virus entry receptor, the angiotensin-converting enzyme 2
59 (ACE2), or expression is restricted to a very small subset of these neurons (Butowt
60 and von Bartheld, 2020; Cooper et al., 2020). Because sustentacular cells tightly
61 enwrap olfactory receptor neurons (Liang, 2020), these ACE2-expressing support cells
62 can easily be mistaken for olfactory receptor neurons, resulting in false positive
63 identification. (2) The timeline of appearance of SARS-CoV-2 in the brain is
64 inconsistent with a “neuron-hopping” mode: infection of third-order olfactory targets
65 should occur with a significant delay after infection of the olfactory epithelium, as has
66 been reported for other neuro-invasive viruses (Barnett et al., 1995), but instead the
67 hypothalamus and brainstem are reported to be infected as early as, or even earlier
68 than, the olfactory bulb (de Melo et al., 2020; Zheng et al., 2020), and SARS-CoV-2
69 may even skip the olfactory nerve and olfactory bulb on its way to brain infection
70 (Winkler et al., 2020; Zhou et al., 2020; Carossino et al., 2021). These findings have
71 raised doubt about the notion that the olfactory nerve serves as a major conduit for
72 brain infection in COVID-19.

73

74 With few exceptions (Briguglio et al., 2020; Butowt and von Bartheld, 2020), studies
75 suggesting an olfactory route for SARS-CoV-2 to achieve brain infection fail to consider
76 an alternative route from the nose to the brain, the route via the nervus terminalis.
77 Many peripheral processes of the nervus terminalis innervate the olfactory epithelium,
78 the blood vessels below this epithelium, as well as cells in Bowman's glands (Larsell,
79 1950), and the central processes of some of these neurons extend to various targets
80 in the forebrain as far caudal as the hypothalamus (Pearson, 1941; Larsell, 1950;
81 Schwanzel-Fukuda et al., 1987; Demski, 1993; von Bartheld, 2004). Some of the
82 nervus terminalis neurons are in direct contact with spaces containing cerebrospinal
83 fluid (CSF) in the region of the olfactory nerve and bulb (Jennes, 1987). About 30-40%
84 of the neurons of the nervus terminalis express gonadotropin-releasing hormone
85 (GnRH) and some of these neurons may release GnRH into blood vessels below the
86 olfactory epithelium (Jennes, 1987; Schwanzel-Fukuda et al., 1987), while other
87 neuronal populations of the nervus terminalis system are thought to regulate blood flow
88 and blood pressure in the nose and forebrain (Larsell, 1918; Oelschläger et al., 1987;
89 Ridgway et al., 1987). These properties make the nervus terminalis a strong candidate
90 for expression of ACE2, known to regulate blood flow and blood pressure in many
91 tissues (Tikellis and Thomas, 2012). Expression of ACE2 in the nervus terminalis
92 would suggest that this cranial nerve is a plausible alternative to the olfactory nerve for
93 SARS-CoV-2 virus to gain access to the brain. However, it has not been previously
94 examined and reported whether nervus terminalis neurons express the obligatory viral
95 entry receptor, ACE2. We have therefore examined whether ACE2 is expressed in
96 these neurons in an animal model, the postnatal mouse.

97

98

99

100 **MATERIALS AND METHODS**

101

102 **Animals and tissue processing**

103 A total of six wildtype C57BL/6J mice (Jackson Laboratory) at age 3-4 weeks old were
104 used to obtain tissue material for experiments. Mice were housed with a 12/12 h
105 light/dark cycle and given access to water and food ad libitum. All animal experiments
106 were approved by the local ethics committee for animal research at Bydgoszcz
107 (Poland). Immediately after cervical dislocation, the mice were exsanguinated and
108 tissues were dissected. Olfactory epithelium and brain were frozen at -80°C for
109 storage and further usage or fixed 3 h at 4°C in 4% (w/v) freshly prepared
110 paraformaldehyde in phosphate-buffered saline (PBS, pH 7,5) and then incubated in
111 25% (w/v) sucrose/PBS at 4°C for 16–24 h, frozen in Tissue-Tek O.C.T. (Sakura
112 Finetek), and cryosectioned at 10-12 μm using a Leica CM1850 cryostat.

113

114 **ACE2 $-/-$ knockout (ACE2 KO) control**

115 To verify the specificity of the ACE2 antibody, an ACE2 knock-out (KO) mouse line
116 was obtained from Taconic (strain #18180). Two male homozygous ACE2 KO mice at
117 age 3 weeks old were processed and immunolabeled as described below for wildtype
118 mice. Genotyping was performed according to the manufacturer's suggested PCR
119 protocol. Lack of an ACE2 protein band was confirmed by using Western blots (not
120 shown).

121

122 **Immunocytochemistry and co-localization analysis**

123 For single immunofluorescence labeling, frozen sections cut at 10-12 μm were stained
124 overnight with a mixture of primary goat anti-ACE2 at 1/500 dilution and rabbit anti-
125 GnRH (gonadotropin releasing hormone) at 4°C . Next day sections were washed five
126 times in PBST (PBS with 0.05% Triton X-100) and incubated with a mixture of
127 secondary anti-rabbit-AF488 antibody and anti-goat-AF594 at 1/500 dilution for 60 min
128 at room temperature. Next, sections were stained for 5 min at room temperature in
129 Hoechst 33258 (Sigma-Aldrich) to visualize cell nuclei and embedded in antifade
130 medium (Vector laboratories). Alternatively, cryosections were stained with rabbit
131 polyclonal anti-CHAT (choline acetyltransferase) instead of rabbit anti-GnRH antibody
132 in the double staining primary antibody mixture. Occasionally, sections were stained

133 with anti-OMP (olfactory marker protein) at 1/500 dilution in PBST, following the same
134 protocol. After immunocytochemical reactions, sections were analyzed on a Nikon
135 Eclipse 80i microscope and images were taken using a Nikon DP80 camera.
136 Microscopic images were processed using CellSense software (Nikon corp).
137 Antibodies used in this study are listed in Supplemental Material, Table S1.

138

139 **Cell counting and statistical analysis**

140 For counting double labeled cells, four male wildtype mice at age 3-4 weeks old were
141 used. Approximately every third coronal cryosection (10-12 μm thickness) was stained
142 as described above, and positive cells were counted in tissue sections under a
143 fluorescent microscope as indicated in Fig. 1 (the medial region from the posterior
144 olfactory epithelium to the caudal end of the olfactory bulb). For each animal, the
145 percentage of double labeled GnRH+/ACE2+ cells was calculated in relation to the
146 total number of GnRH-positive cells detected. The same protocol was applied for
147 counting cholinergic nervus terminalis neurons co-labeled with ACE2. A total number
148 of approximately 100 GnRH-positive neurons and 50 CHAT-positive neurons were
149 counted from four animals. The results were analyzed using GraphPad Prism software.
150 Results are presented as mean \pm SEM.

151

152 **RESULTS**

153

154 It was previously shown that GnRH is a marker for a major fraction of nervus terminalis
155 neurons (Jennes, 1987; Schwanzel-Fukuda et al., 1987; Demski, 1993; Kim et al.,
156 1999; von Bartheld, 2004). Immunolabeling for GnRH in 3-4 week-old mice showed
157 labeled cells localized along the olfactory nerve between the olfactory epithelium and
158 the olfactory bulbs (Fig. 2A-H), as expected from previous studies in rodents
159 (Schwanzel-Fukuda et al., 1986; Wirsig and Leonard, 1986; Schwanzel-Fukuda et al.,
160 1987). The majority of the GnRH-positive nervus terminalis neurons was located along
161 the midline in the posterior part of the olfactory epithelium and adjacent to the olfactory
162 bulbs. Preliminary examination revealed that these cells were in the same vicinity as
163 cells labeled with the ACE2 antibody (Fig. 2A-B, E-F). The large majority of GnRH-
164 positive nervus terminalis neurons were fusiform and unipolar in shape.

165

166 **Double-label of GnRH and ACE2 neurons with quantification**

167 In order to determine whether some neurons of the nervus terminalis contained both
168 GnRH and ACE2, and to estimate the number of such cells, we performed double
169 immunolabeling experiments, and single- and double-labeled cells were counted on
170 15-20 sections from three different animals. The analyzed olfactory epithelium and
171 olfactory bulb region and section's cutting plane are as indicated in Fig. 1. After
172 counting a total of 107 double positive (GnRH+/ACE2+) cells it was calculated that
173 90.9% of them were double-labeled (Fig. 3). Controls included omission of the primary
174 antibody (not shown) and double immunofluorescent reactions performed using
175 cryosections derived from an ACE2 knockout mouse as shown in Fig. 2 (I-L). The
176 GnRH-positive cells were never positive for olfactory marker protein (OMP), a marker
177 for mature olfactory receptor neurons (Fig. S1, supplementary materials). The total
178 number of GnRH+ nervus terminalis neurons per mouse was estimated to be
179 approximately 125, which is very similar to a previous serial section analysis in hamster
180 (about 130-140 GnRH+ neurons, Wirsig and Leonard, 1986).

181

182 **Double-label of CHAT and ACE2 neurons with quantification**

183 The nervus terminalis complex is comprised of several distinct heterogenic populations
184 of neurons. In addition to GnRH cells which form the majority of nervus terminalis cells,
185 the second largest nervus terminalis subpopulation are cholinergic neurons that can

186 be identified by the presence of choline acetyltransferase (CHAT) or cholinesterase
187 (Wirsig and Leonard, 1986; Demski, 1993; von Bartheld, 2004). Therefore, CHAT
188 neurons were also double labeled with ACE2 and the fraction of CHAT-positive and
189 ACE2-positive neurons was estimated out of a total of 51 CHAT-positive neurons in
190 four animals. In contrast to GnRH+/ACE2+ cells, only a minor fraction of about 9.4%
191 of CHAT-positive cells were labeled with ACE2 which suggests that very few
192 cholinergic nervus terminalis cells express ACE2 protein (Fig. 3). The large majority of
193 CHAT-positive and also ACE2-positive nervus terminalis neurons were fusiform and
194 unipolar in shape. Control experiments included omission of primary antibody (not
195 shown) and double immunofluorescent reactions performed using cryosections
196 derived from ACE2 knockout mouse (see below). The total number of CHAT-positive
197 nervus terminalis neurons per mouse was estimated to be approximately 60-70. This
198 is less than the 130-140 acetylcholinesterase containing nervus terminalis neurons in
199 hamster (Wirsig and Leonard, 1986), but it is known that only a fraction of neurons
200 containing acetylcholinesterase actually are cholinergic (Schwanzel-Fukuda et al.,
201 1986).

202

203 **Knock-out control mice for ACE2 -/-**

204 Immunolabeling experiments did not reveal any signal beyond background when the
205 primary antibodies were omitted. For more precise visualization of background ACE2
206 staining, tissue derived from ACE2 knock-out mouse was used. Experiments using
207 Western blotting technique showed lack of an ACE2-specific band in total protein
208 extract obtained from ACE2 -/- animals (results not shown). Therefore, these sections
209 were also used for double immunolabeling experiments with ACE2 antibody and
210 results showed that, as expected, GnRH-positive cells were negative for ACE2 in
211 tissue sections from the knock-out animals (Fig. 2 I-L).

212

213

214

215 **DISCUSSION**

216

217 Our experiments confirmed the locations and approximate numbers of GnRH-positive
218 neurons of the nervus terminalis in rodents (Schwanzel-Fukuda et al., 1986; Wirsig
219 and Leonard, 1986; Schwanzel-Fukuda et al., 1987). In mouse, we found that the
220 number of CHAT-positive neurons was about half of the number of GnRH-positive
221 neurons. Interestingly, the large majority of GnRH-positive neurons also expressed
222 ACE2, while only a small fraction of CHAT-positive neurons co-localized ACE2.
223 Previous studies have suggested that the CHAT-positive neurons more often were
224 multipolar and possibly associated with an autonomic function, such as innervating
225 Bowman glands, while GnRH-positive neurons were thought to be sensory and/or may
226 have neurosecretory functions (Wirsig and Leonard, 1986; Schwanzel-Fukuda et al.,
227 1986).

228

229 Mice have been most often used as model systems for ACE2 expression, for
230 localization of SARS-CoV-2 in the olfactory epithelium, and to study neuro-invasion of
231 the brain along the olfactory route (Butowt and von Bartheld, 2020; Cooper et al., 2020;
232 Rathnasinghe et al., 2020). Mice have the advantage that a large number of mutants
233 are available (Butowt and von Bartheld, 2020), but they normally express an ACE2
234 version that binds SARS-CoV-2 with low affinity (Damas et al., 2020). Therefore, to
235 study SARS-CoV-2 infection in mice, a mouse-adapted virus has to be used (Leist et
236 al., 2020), or mice have to be engineered to express human ACE2.

237

238 Importantly, our finding of ACE2 expression in the large majority of GnRH-expressing
239 nervus terminalis neurons suggests that this cranial nerve is a more plausible conduit
240 for brain infection than the olfactory neurons that entirely or for the most part lack ACE2
241 expression (Butowt and von Bartheld, 2020; Cooper et al., 2020). The nervus terminalis
242 neurons may obtain the SARS-CoV-2 directly from infected cells in Bowman's glands,
243 or through free nerve endings within the olfactory epithelium, many parts of which
244 degenerate when sustentacular cells are infected by SARS-CoV-2 (Bryche et al.,
245 2020). As illustrated in Fig. 4, the nervus terminalis thus has multiple venues to bind
246 the virus, while the lack of ACE2 in olfactory receptor neurons appears to be a barrier
247 to virus transfer.

248

249 Another important aspect is that the timeline of appearance of SARS-CoV-2 in the
250 brain fits the nervus terminalis projections, with an explosive appearance of the virus
251 in the forebrain in some mouse models (Winkler et al., 2020; Zheng et al., 2020; Zhou
252 et al., 2020; Carossino et al., 2021), rather than a gradual transfer along the olfactory
253 projections as would be expected from a virus that gains access to the brain via
254 olfactory projections (Barnett and Perlman, 1993). The nervus terminalis has direct
255 projections into the forebrain, reaching as far caudal as the hypothalamus (von
256 Bartheld, 2004), and this could explain why the virus reaches the brain and
257 cerebrospinal fluid (CSF) spaces much faster than seems possible via “neuron
258 hopping” along olfactory projections. Most of the virus-containing axons in the olfactory
259 nerve demonstrated by Melo et al. (2020) do not express olfactory marker protein,
260 suggesting that they are not axons belonging to olfactory receptor neurons, and
261 therefore may be nervus terminalis axons which also project through the olfactory
262 nerve (Larsell, 1950).

263

264 On a comparative note, since dolphins and whales have a much larger number of
265 nervus terminalis cells than any other vertebrates (Oelschläger et al., 1987), and these
266 marine mammals express ACE2 that is highly susceptible to SARS-CoV-2 infection
267 (Damas et al., 2020), our finding of ACE2 in nervus terminalis cells suggests that these
268 animals may be more vulnerable to brain infection via the nervus terminalis – even in
269 the absence of an olfactory system.

270

271 In humans, the number of nervus terminalis neurons is relatively small (a few hundred
272 to a few thousand neurons depending on age, Brookover, 1917; Larsell, 1950; Jin et
273 al., 2019). However, such a relatively small number may be sufficient to mediate viral
274 infection, especially considering that the nervus terminalis directly innervates secretory
275 cells of the Bowman’s glands (Larsell, 1950) that are known to express ACE2 (Brann
276 et al., 2020; Chen et al., 2020; Cooper et al., 2020; Ye et al., 2020; Zhang et al., 2020;
277 Klingenstein et al., 2021) and readily become infected with SARS-CoV-2 (Ye et al.,
278 2020; Leist et al., 2020; Meinhardt et al., 2020; Zhang et al., 2020; Zheng et al., 2020)
279 (Fig. 4). In addition, the nervus terminalis has many free nerve endings within the
280 olfactory epithelium (Larsell, 1950) – an epithelium that is heavily damaged when
281 ACE2-expressing sustentacular cells become infected and degenerate (Bryche et al.,

282 2020). Finally, a major component of the nervus terminalis innervates blood vessels
283 below the olfactory epithelium and projects via cerebrospinal fluid (CSF)-containing
284 spaces (Larsell, 1950; Jennes, 1987). Some nervus terminalis neurons have direct
285 projections to the hypothalamus (Pearson, 1941; Larsell, 1950; von Bartheld, 2004), a
286 brain region that may serve as a hub for virus spread throughout the brain (Nampoothiri
287 et al., 2020; Zheng et al., 2020).

288

289 Another argument to consider the nervus terminalis as an alternative to the olfactory
290 route is that neuro-invasion in most animal models is highly variable, even in the same
291 species and transgenic model (Jiang et al., 2020; Oladunni et al., 2020; Rathnasinghe
292 et al., 2020; Winkler et al., 2020; Ye et al., 2020; Zheng et al., 2020; Zhou et al., 2020),
293 and this is despite a very consistent olfactory system in terms of numbers of neurons,
294 gene expression and projections. The nervus terminalis, on the other hand, is known
295 for its unusually large variability between individuals of the same species or even when
296 comparing the right side with the left side of the same individual (Larsell, 1918; Jin et
297 al., 2019). Such numerical differences can approach or even exceed an entire order of
298 magnitude (Schwanzel-Fukuda et al., 1987; Jin et al., 2019) – and thus may explain
299 the reported large variability in neuro-invasion along this route. Taken together, nervus
300 terminalis neurons, for the above reasons, should be considered as a plausible
301 alternative to the olfactory projections for neuro-invasion of SARS-CoV-2 from the
302 nose to the brain in COVID-19.

303

304

305 **ACKNOWLEDGMENTS**

306 Supported by the “Excellence Initiative-Research University” programme at the
307 Nicolaus Copernicus University (R.B.), and grant GM103554 from the National
308 Institutes of Health (C.S.v.B.).

309

310

311 **CONTRIBUTION TO THE FIELD**

312

313 The new coronavirus responsible for the COVID-19 pandemic can infect the brain in
314 humans and in some animal models. It is currently not known how this virus infects the
315 brain. Many researchers believe that the virus enters the brain by using a route along
316 the olfactory nerve. However, the olfactory neurons in the nose do not express the
317 obligatory virus entry receptor, and the timing of arrival and transfer of the virus in brain
318 targets is inconsistent with a neuronal transfer along olfactory projections. Here we
319 show that an alternative route for the new coronavirus to infect the brain is more
320 plausible. We show that many nervus terminalis neurons express the obligatory virus
321 entry protein. Since these neurons have direct contact with cells known to become
322 infected in the nose, and have direct projections to various targets in the forebrain, the
323 nervus terminalis neurons provide an alternative route for the new coronavirus to gain
324 access from the nose to the brain.

325

326 **REFERENCES**

327
328
329
330
331
332
333
334
335
336
337
338
339
340
341
342
343
344
345
346
347
348
349
350
351
352
353
354
355
356
357
358
359
360
361
362
363
364
365
366
367
368
369
370
371
372
373
374

Barnett, E.M., and Perlman, S. (1993). The olfactory nerve and not the trigeminal nerve is the major site of CNS entry for mouse hepatitis virus, strain JHM. *Virology*. 194(1), 185-191.

Barnett, E.M., Evans, G.D., Sun, N., Perlman, S., and Cassell, M.D. (1995). Anterograde tracing of trigeminal afferent pathways from the murine tooth pulp to cortex using herpes simplex virus type 1. *J Neurosci*. (4), 2972-2984.

Bilinska, K., Jakubowska, P., Von Bartheld, C.S., and Butowt, R. (2020). Expression of the SARS-CoV-2 Entry Proteins, ACE2 and TMPRSS2, in Cells of the Olfactory Epithelium: Identification of Cell Types and Trends with Age. *ACS Chem Neurosci*. 11(11), 1555-1562.

Bougakov, D., Podell, K., and Goldberg, E. (2020). Multiple Neuroinvasive Pathways in COVID-19. *Mol Neurobiol*. 29,1–12.

Briguglio, M., Bona, A., Porta, M., Dell'Osso, B., Pregliasco, F.E., and Banfi, G. (2020). Disentangling the hypothesis of host dysosmia and SARS-CoV-2: The bait symptom that hides neglected neurophysiological routes. *Front Physiol*. 11, 671.

Brann, D.H., Tsukahara, T., Weinreb, C., Lipovsek, M., Van den Berge, K., Gong, B., et al. (2020). Non-neuronal expression of SARS-CoV-2 entry genes in the olfactory system suggests mechanisms underlying COVID-19-associated anosmia. *Sci Adv*. 6(31):eabc5801.

Brookover, C. (1917). The peripheral distribution of the nervus terminalis in an infant. *J Comp Neurol*. 28, 349-360.

Bryche, B., St Albin, A., Murri, S., Lacôte, S., Pulido, C., Ar Gouilh, M., et al. (2020). Massive transient damage of the olfactory epithelium associated with infection of sustentacular cells by SARS-CoV-2 in golden Syrian hamsters. *Brain Behav Immun*. 89, 579-586.

Burks, S.M., Rosas-Hernandez, H., Alenjandro Ramirez-Lee, M., Cuevas, E., and Talpos, J.C. (2021). Can SARS-CoV-2 infect the central nervous system via the olfactory bulb or the blood-brain barrier? *Brain Behav Immun*. 20, 32489-32492.

Butowt, R., and Bilinska, K. (2020). SARS-CoV-2: Olfaction, Brain Infection, and the Urgent Need for Clinical Samples Allowing Earlier Virus Detection. *ACS Chem Neurosci*. 11(9),1200-1203.

Butowt, R., and von Bartheld, C.S. (2020). Anosmia in COVID-19: Underlying Mechanisms and Assessment of an Olfactory Route to Brain Infection. *Neuroscientist*. doi: 10.1177/1073858420956905. Epub ahead of print.

- 375 Carossino, M., Montanaro, P., O'Connell, A., Kenney, D., Gertje, H., Grosz, K.A., et al.
376 (2021). Fatal neuroinvasion of SARS-CoV-2 in K18-hACE2 mice is partially dependent
377 on hACE2 expression. *bioRxiv [Preprint]* doi: 10.1101/2021.01.13.425144. (accessed
378 on February 26, 2021).
- 379
380 Chen, M., Shen, W., Rowan, N. R., Kulaga, H., Hillel, A., Ramanathan, M., Jr, et al.
381 (2020). Elevated ACE-2 expression in the olfactory neuroepithelium: implications for
382 anosmia and upper respiratory SARS-CoV-2 entry and replication. *Eur Resp J.* 56(3),
383 2001948.
- 384
385 Cooper, K.W., Brann, D.H., Farruggia, M.C., Bhutani, S., Pellegrino, R., Tsukahara, T.,
386 et al. (2020). COVID-19 and the Chemical Senses: Supporting Players Take Center
387 Stage. *Neuron.* 107(2), 219-233.
- 388
389 Damas, J., Hughes, G.M., Keough, K.C., Painter, C.A., Persky, N.S., Corbo, M., et al.
390 (2020). Broad host range of SARS-CoV-2 predicted by comparative and structural
391 analysis of ACE2 in vertebrates. *Proc Natl Acad Sci U S A.* 117(36), 22311-22322.
- 392
393 de Melo, G.D., Lazarini, F., Levallois, S., Hautefort, C., Michel, V., Larrous, F., et al.
394 (2020). COVID-19 associated olfactory dysfunction reveals SARS-CoV-2
395 neuroinvasion and persistence in the olfactory system. *bioRxiv [Preprint]*
396 <https://doi.org/10.1101/2020.11.18.388819>. (accessed on February 27, 2021).
- 397
398 Demski, L.S. (1993). Terminal nerve complex. *Acta Anat (Basel).* 148(2-3), 81-95.
- 399
400 Dubé, M., Le Coupand, A., Wong, A.H.M., Rini, J.M., Desforges, M., and Talbot, P.J.
401 (2018). Axonal Transport Enables Neuron-to-Neuron Propagation of Human
402 Coronavirus OC43. *J Virol.* 92(17), 404-418.
- 403
404 Ellul, M.A., Benjamin, L., Singh, B., Lant, S., Michael, B.D., Easton, A., et al. (2020).
405 Neurological associations of COVID-19. *Lancet Neurol.* 19(9), 767-783.
- 406
407 Jennes, L. (1987). The nervus terminalis in the mouse: light and electron microscopic
408 immunocytochemical studies. *Ann N Y Acad Sci.* 519,165-173.
- 409
410 Jiang, R. D., Liu, M. Q., Chen, Y., Shan, C., Zhou, Y. W., Shen, X. R., et al. (2020).
411 Pathogenesis of SARS-CoV-2 in Transgenic Mice Expressing Human Angiotensin-
412 Converting Enzyme 2. *Cell.* 182(1), 50–58.e8.
- 413
414 Jin, Z.W., Cho, K.H., Shibata, S., Yamamoto, M., Murakami, G., and Rodríguez-
415 Vázquez, J.F. (2019). Nervus terminalis and nerves to the vomeronasal organ: a study
416 using human fetal specimens. *Anat Cell Biol.* 52(3), 278-285.
- 417
418 Kim, K.H., Patel, L., Tobet, S.A., King, J.C., Rubin, B.S., and Stopa, E.G. (1999).
419 Gonadotropin-releasing hormone immunoreactivity in the adult and fetal human
420 olfactory system. *Brain Res.* 826(2), 220-229.
- 421
422 Klingenstein, M., Klingenstein, S., Neckel, P.H., Mack, A.F., Wagner, A.P, Kleger, A.,
423 et al. (2021). Evidence of SARS-CoV2 Entry Protein ACE2 in the Human Nose and
424 Olfactory Bulb. *Cells Tissues Organs E-pub.* doi: 10.1159/000513040

- 425 Larsell, O. (1918). Nervus terminalis: mammals. *J Comp Neurol.* 30, 3-68.
426
- 427 Larsell, O. (1950). The nervus terminalis. *Ann Otol Rhinol Laryngol.* 59(2), 414-438.
428
- 429 Leist, S.R., Dinnon, K.H., Schäfer, A., Tse, L.V., Okuda, K., Hou, Y.J., et al. (2020). A
430 Mouse-Adapted SARS-CoV-2 Induces Acute Lung Injury and Mortality in Standard
431 Laboratory Mice. *Cell.* 183 (4),1070-1085.
432
- 433 Li, Z., Liu, T., Yang, N., Han, D., Mi, X., Li, Y., et al. (2020). Neurological manifestations
434 of patients with COVID-19: potential routes of SARS-CoV-2 neuroinvasion from the
435 periphery to the brain. *Front Med.* 14(5), 533-541.
436
- 437 Liang, F. (2020). Sustentacular Cell Enwrapment of Olfactory Receptor Neuronal
438 Dendrites: An Update. *Genes (Basel).* 11(5), 493.
439
- 440 Matschke, J., Lütgehetmann, M., Hagel, C., Sperhake, J.P., Schröder, A.S., Edler, C.,
441 et al. (2020). Neuropathology of patients with COVID-19 in Germany: a post-mortem
442 case series. *Lancet Neurol.* 19(11), 919-929.
443
- 444 Meinhardt, J., Radke, J., Dittmayer, C., Franz, J., Thomas, C., Mothes, R., et al. (2020).
445 Olfactory transmucosal SARS-CoV-2 invasion as a port of central nervous system
446 entry in individuals with COVID-19. *Nat Neurosci.* doi: 10.1038/s41593-020-00758-5
447
- 448 Mukerji, S.S., and Solomon, I.H. (2020). What can we learn from brain autopsy in
449 COVID-19? *Neurosci Lett.* 135528. doi: 10.1016/j.neulet.2020.135528
450
- 451 Nampoothiri, S., Sauve, S., Ternier, G., Fernandois, D., Coelho, C., Imbernon, M., et
452 al. (2020). The hypothalamus as a hub for putative SARS-CoV-2 brain infection.
453 *bioRxiv [Preprint]* doi: <https://doi.org/10.1101/2020.06.08.139329>. (accessed on
454 February 27, 2021)
455
- 456 Natoli, S., Oliveira, V., Calabresi, P., Maia, L.F., and Pisani, A. (2020). Does SARS-
457 Cov-2 invade the brain? Translational lessons from animal models. *Eur J Neurol.*
458 9,1764-1773.
459
- 460 Netland, J., Meyerholz, D.K., Moore, S., Cassell, M., and Perlman, S. (2008). Severe
461 acute respiratory syndrome coronavirus infection causes neuronal death in the
462 absence of encephalitis in mice transgenic for human ACE2. *J Virol.* 82(15), 7264-
463 7275.
464
- 465 Oelschläger, H.A., Buhl, E.H., and Dann, J.F. (1987). Development of the nervus
466 terminalis in mammals including toothed whales and humans. *Ann N Y Acad Sci.* 519,
467 447-464.
468
- 469 Oladunni, F. S., Park, J. G., Pino, P. A., Gonzalez, O., Akhter, A., Allué-Guardia, A., et
470 al. (2020). Lethality of SARS-CoV-2 infection in K18 human angiotensin-converting
471 enzyme 2 transgenic mice. *Nat Commun.* 11(1), 6122.
472
- 473 Pearson, A.A. (1941). The development of the nervus terminalis in man. *J Comp*
474 *Neurol.* 75, 39-66.

475
476 Rathnasinghe, R., Strohmeier, S., Amanat, F., Gillespie, V.L., Krammer, F., García-
477 Sastre, A., et al. (2020). Comparison of transgenic and adenovirus hACE2 mouse
478 models for SARS-CoV-2 infection. *Emerg Microbes Infect.* 1, 2433-2445.
479
480 Ridgway, S.H., Demski, L.S., Bullock, T.H., and Schwanzel-Fukuda, M. (1987). The
481 terminal nerve in odontocete cetaceans. *Ann N Y Acad Sci.* 519, 201-212.
482
483 Schwanzel-Fukuda, M., Morrell, J. I., and Pfaff, D. W. (1986). Localization of choline
484 acetyltransferase and vasoactive intestinal polypeptide-like immunoreactivity in the
485 nervus terminalis of the fetal and neonatal rat. *Peptides.* 7(5), 899–906.
486
487 Schwanzel-Fukuda, M., Garcia, M.S., Morrell, J.I., and Pfaff, D.W. (1987). Distribution
488 of luteinizing hormone-releasing hormone in the nervus terminalis and brain of the
489 mouse detected by immunocytochemistry. *J Comp Neurol.* 255(2), 231-244.
490
491 Solomon, T. (2021). Neurological infection with SARS-CoV-2 - the story so far. *Nat*
492 *Rev Neurol.* 1–2.
493
494 Tikellis, C., and Thomas, M.C. (2012). Angiotensin-Converting Enzyme 2 (ACE2) Is a
495 Key Modulator of the Renin Angiotensin System in Health and Disease. *Int J Pept.*
496 2012:256294.
497
498 van Riel, D., Verdijk, R., and Kuiken, T. (2015). The olfactory nerve: a shortcut for
499 influenza and other viral diseases into the central nervous system. *J Pathol.* 235(2),
500 277-287.
501
502 von Bartheld, C.S. (2004). The terminal nerve and its relation with extrabulbar
503 "olfactory" projections: lessons from lampreys and lungfishes. *Microsc Res Tech.* 65(1-
504 2),13-24.
505
506 Winkler, E. S., Bailey, A. L., Kafai, N. M., Nair, S., McCune, B. T., Yu, J., et al. (2020).
507 SARS-CoV-2 infection of human ACE2-transgenic mice causes severe lung
508 inflammation and impaired function. *Nat Immunol.* 21(11), 1327–1335.
509
510 Wirsig, C.R., and Leonard, C.M. (1986). Acetylcholinesterase and luteinizing hormone-
511 releasing hormone distinguish separate populations of terminal nerve neurons.
512 *Neuroscience,* 19(3), 719–740.
513
514 Ye, Q., Zhou, J., Yang, G., Li, R.-T., He, Q., Zhang, Y., et al. (2020). SARS-CoV-2
515 infection causes transient olfactory dysfunction in mice. *bioRxiv [Preprint]* doi:
516 <https://doi.org/10.1101/2020.11.10.376673>. (accessed on February 26, 2021).
517
518 Zhang, A.J., Lee, A.C., Chu, H., Chan, J.F., Fan, Z., Li, C., et al. (2020). SARS-CoV-2
519 infects and damages the mature and immature olfactory sensory neurons of hamsters.
520 *Clin Infect Dis.* 15:ciaa995. doi: 10.1093/cid/ciaa995
521
522 Zheng, J., Wong, L.R., Li, K., Verma, A.K., Ortiz, M., Wohlford-Lenane, C., et al.
523 (2021). COVID-19 treatments and pathogenesis including anosmia in K18-hACE2
524 mice. *Nature* 589, 603–607.

525

526 Zhou, B., Thao, T.T.N., Hoffmann, D., Taddeo, A., Ebert, N., Labroussaa, F., et al.
527 (2020). SARS-CoV-2 spike D614G variant confers enhanced replication and
528 transmissibility. bioRxiv [Preprint]. doi: 10.1101/2020.10.27.357558. (accessed on
529 February 26, 2021).

530

531 Zubair, A.S., McAlpine, L.S., Gardin, T., Farhadian, S., Kuruvilla, D.E., and Spudich,
532 S. (2020). Neuropathogenesis and Neurologic Manifestations of the Coronaviruses in
533 the Age of Coronavirus Disease 2019: A Review. JAMA Neurol. 77(8), 1018-1027.

534

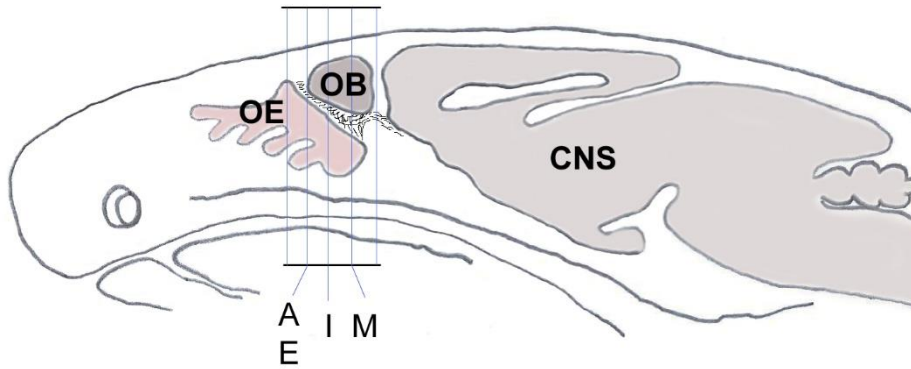
535

536 **FIGURES AND FIGURE LEGENDS**

537

538

539



540

541

542 **Fig. 1.** Schematic sagittal section through a mouse head shows the orientation and
543 planes of tissue sections from Fig. 2A, E, I and M that were used for demonstration of
544 double-immunolabeling and cell counting.

545

546

547

548

549

550

551

552

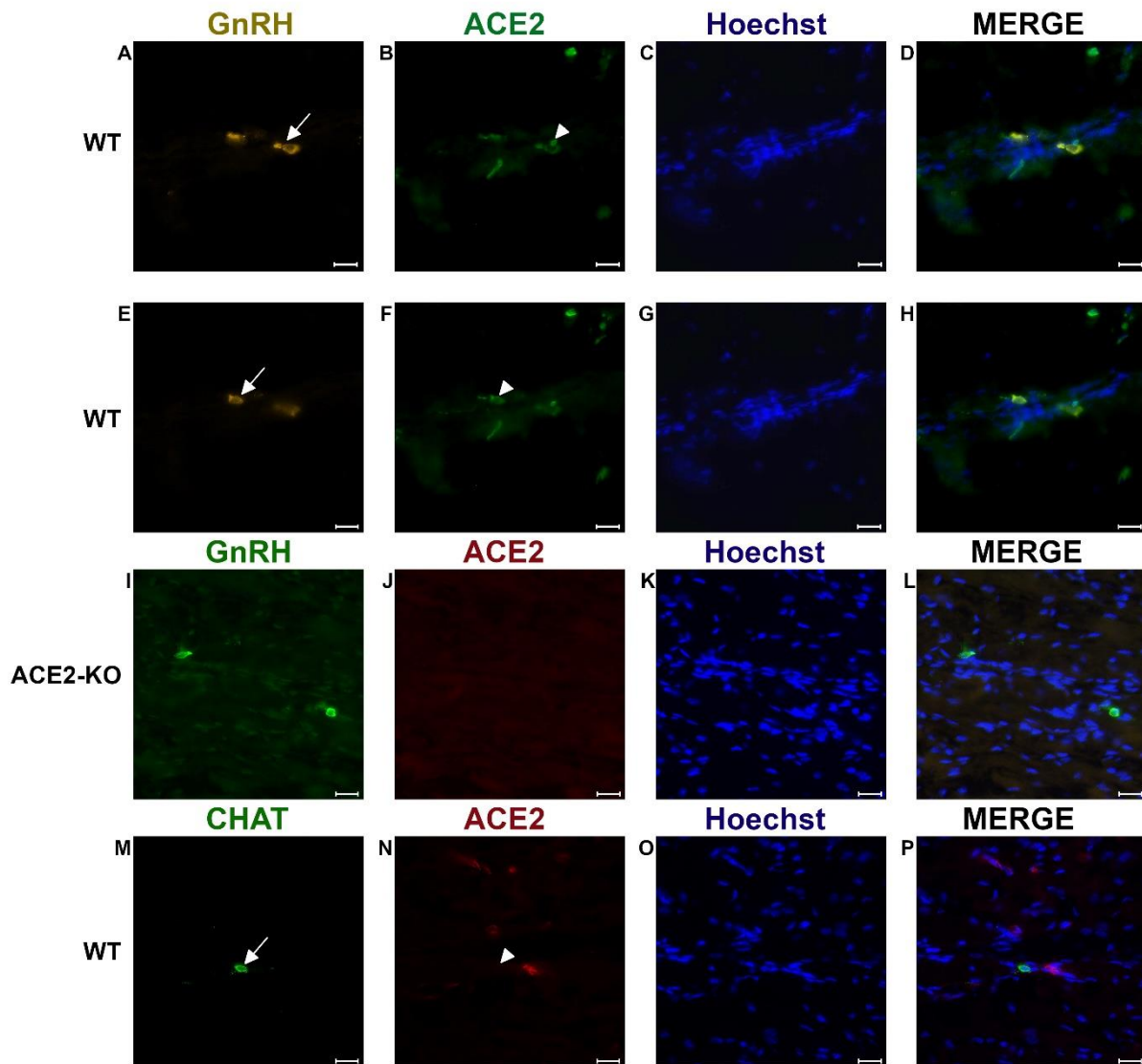
553

554

555

556

557

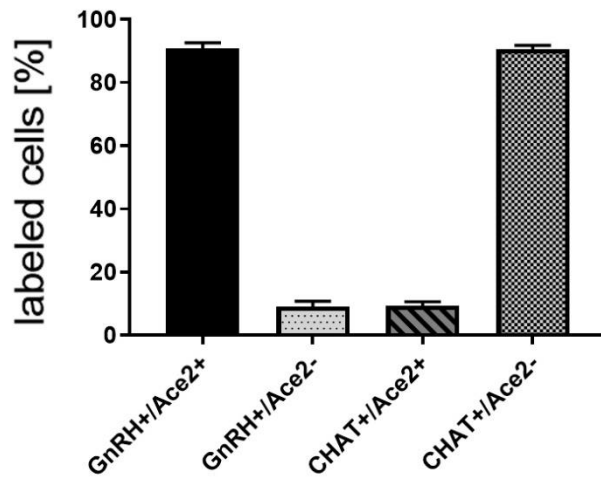


558

559 **Fig. 2.** Examples of double immunofluorescent labeling for nervus terminalis
560 neuronal markers GnRH (A, E) or CHAT (M) and ACE2 (B, F, J, N) in the medial
561 region adjacent to the olfactory bulbs as indicated in Fig. 1. Panels A-D and E-H
562 show slightly different focal planes to demonstrate the morphology of the two or three
563 different neurons. Nuclei are stained with Hoechst 33258 (C, G, K, O). Merged
564 images are shown in the last column (D, H, L, P). The neuronal somas labeled with
565 GnRH (A, E) are co-labeled with ACE2 (B, F) as shown after merging (D, H). GnRH
566 positive cells in the ACE2 knock-out mouse (I) are not labeled with ACE2 (J). The
567 majority of cholinergic neurons are not labeled with ACE2 (M, N), as quantified in Fig.
568 3. Control sections probed without primary antibodies or with control rabbit IgG had
569 no detectable signal (not shown). Arrows and triangles indicate double-labeled
570 neurons or lack thereof. Scale bars: 20 μ m.

571

572



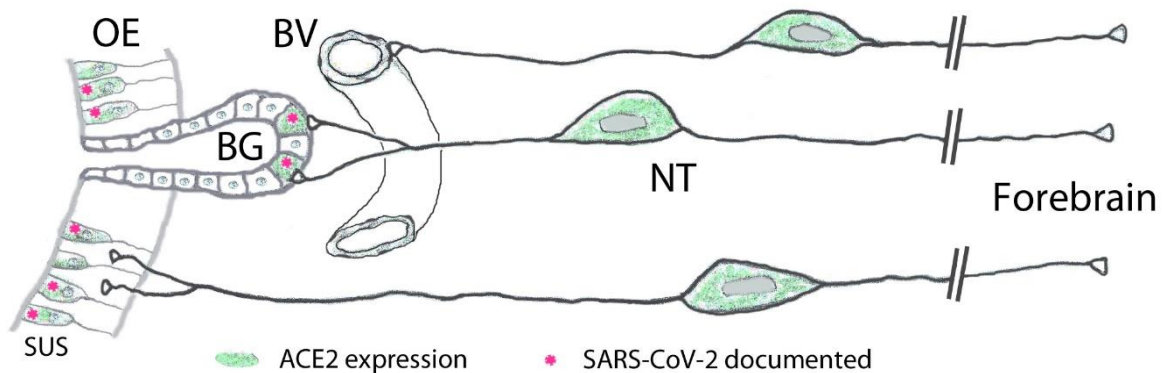
573

574

575 **Fig. 3.** Quantification of co-localization of GnRH and ACE2, and CHAT and ACE2 in
576 nervus terminalis neurons. The large majority of GnRH-positive neurons is also
577 ACE2-positive. In contrast, the majority of CHAT-positive (cholinergic) nervus
578 terminalis neurons lack ACE2-expression. The total number of counted GnRH-
579 positive or CHAT-positive neurons was set at 100%. Error bars represent \pm SEM.

580

581



582

583

584 **Fig. 4.** Peripheral projections of nervus terminalis (NT) neurons and their
585 presumptive relationship with ACE2-expressing neurons in the olfactory epithelium
586 and known SARS-CoV-2 infection. NT neurons innervate blood vessels (BV),
587 Bowman gland (BG) cells, and the olfactory epithelium (OE). Peripheral projections of
588 NT neurons according to Larsell (1950). Cells expressing ACE2 are indicated in
589 green, including sustentacular cells (SUS) and BG cells. Both of these cell types
590 have been shown to express ACE2 (Bilinska et al., 2020; Brann et al., 2020; Chen et
591 al., 2020; Ye et al., 2020; Zhang et al., 2020; Klingenstein et al., 2021). Cell types
592 that have been documented to be infected by SARS-CoV-2 are indicated with pink
593 asterisks. SARS-CoV-2 localization in SUS cells according to Bryche et al., 2020; de
594 Melo et al., 2020; Leist et al., 2020; Ye et al., 2020; Zhang et al., 2020; Zheng et al.,
595 2020, and in BG cells according to Bryche et al., 2020; Leist et al., 2020; Ye et al.,
596 2020.

597

598

599 **SUPPLEMENTARY MATERIAL**

600

601 **SUPPLEMENTAL TABLES**

602

603 **Table S1.** Primary and secondary antibodies used in this study.

604

Primary antibodies	Company	Cat. #	Type
ACE2	R&D Systems	AF3437	goat polyclonal
GnRH1	Proteintech	26950-1-AP	rabbit polyclonal
CHAT	Proteintech	24418-1-AP	rabbit polyclonal
OMP	WAKO	544-10001	goat polyclonal
Secondary antibodies			Fluorescent conjugate
donkey anti-rabbit	Abcam	ab15006	AF488
donkey anti-goat	Abcam	ab150136	AF594

605

606 Abbreviations: ACE2, angiotensin converting enzyme 2; CHAT, choline acetyltransferase; GnRH1,
607 gonadotropin releasing hormone 1; OMP, olfactory marker protein.

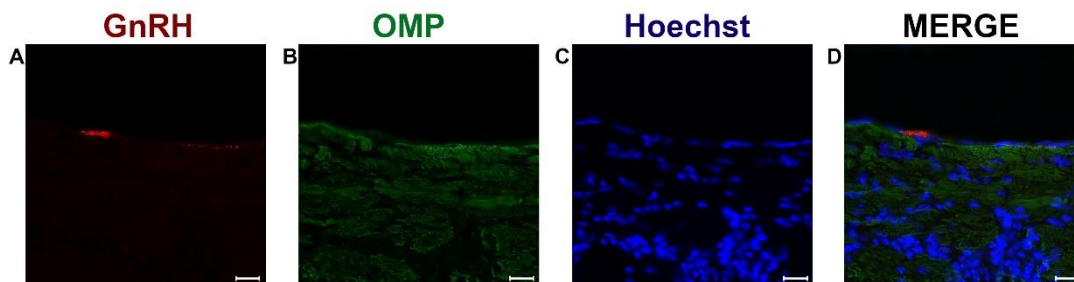
608

609

610

611 **SUPPLEMENTAL FIGURES**

612



613

614

615 **Fig. S1.** Example of double immunofluorescent labeling for nervus terminalis neuronal
616 markers GnRH (A) and olfactory marker protein (OMP) (B) in the medial region
617 adjacent to the olfactory bulbs as indicated in Fig. 1. Nuclei are stained with Hoechst
618 33258 (C) and the merged image is shown in (D). GnRH-labeled cells were never
619 labeled for OMP in this region. Scale bars: 20 μ m.

620